Transfer Learning for Continuous Blood Pressure Change: Personalizing for SCI Individuals during Autonomic Dysregulation Episodes

Itilekha Podder, Udo Bub, Robert Riener, Jürgen Pannek, Inge Eriks-Hoogland and Diego Paez-Granados, Member, IEEE

S0. Extended Data Preprocessing

Raw PPG and ECG signals were segmented into fixed-length 5-second windows around each available blood pressure (BP) measurement. PPG signals were denoised using a fourth-order Butterworth bandpass filter (0.25–10 Hz) and baseline-corrected using adaptive iteratively reweighted penalized least squares (airPLS) [1]. Beat-to-beat segmentation was performed via extrema detection. Segments with fewer than five valid beats were discarded, and remaining beats were min-max normalized. ECG signals were denoised using wavelet decomposition with the bior4.4 wavelet, with decomposition levels selected adaptively to preserve QRS, P-, and T-wave morphology. ECG segments were also scaled to the [0,1] range via min-max normalization. Each segmented window underwent morphological and rhythm-based quality checks. Template matching using Euclidean distance was performed against canonical beat shapes. Segments failing to meet quality thresholds were excluded, ensuring inclusion of only physiologically valid beat patterns. Continuous wavelet transform (CWT) was used to convert temporal signals into time–frequency representations. We used the Morlet mother wavelet [2] and computed the log-magnitude of CWT coefficients to generate scalograms. This approach is well-suited for capturing transient spectral features such as heart rate variability and respiratory harmonics, particularly under autonomic dysregulation. Scalograms enhance the performance of convolutional models and have shown improved generalization and interpretability in biomedical signal modelling [3].

TABLE I: Blood pressure grouping criteria

Category	SBP Range (mmHg)	DBP Range (mmHg)
Normal	< 120	and < 80
Elevated	[120, 130)	and < 80
Hypertension S1	[130, 140)	or [80, 90)
Hypertension S2	≥ 140	or ≥ 90

Demographic features were filtered based on a signal quality threshold (≤ 0.65), normalized, and appropriately encoded. Samples with missing baseline or current BP values were excluded. PPG, ECG, and demographic data were used to estimate systolic BP changes (ΔSBP). Baseline BP values were stratified into four clinical categories—Normal, Elevated, Hypertension Stage 1, and Hypertension Stage 2—based on ACC/AHA guidelines [4], as summarized in Table I.
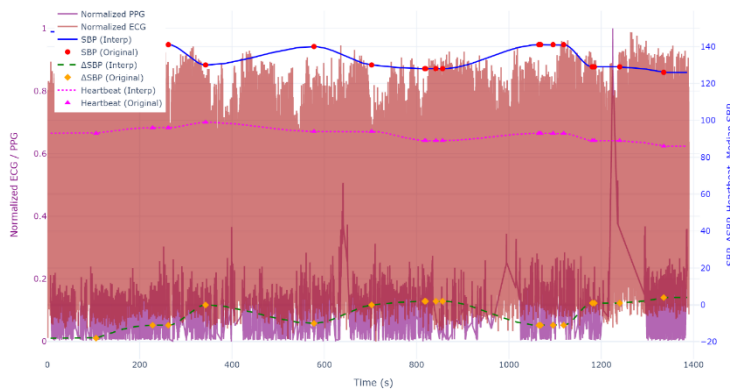
To align high-resolution physiological signals with sparse BP annotations, Akima spline interpolation was applied to SBP, ΔSBP, heart rate, and baseline SBP, matching the temporal resolution of the PPG waveform. Akima was chosen for its ability to handle irregular data without introducing oscillations. Nearest-neighbor extrapolation ensured label continuity at signal boundaries. This enabled frame-level supervision while maintaining physiological plausibility. Interpolation was particularly important for the SCI dataset, where BP annotations were sparse and unevenly distributed. In many cases, only a few valid readings were available per session, making direct time-series modelling infeasible. Interpolation generated continuous supervisory labels, enabling effective multimodal data fusion. Visual inspection (see the figure above) confirmed alignment quality and signal coherence.

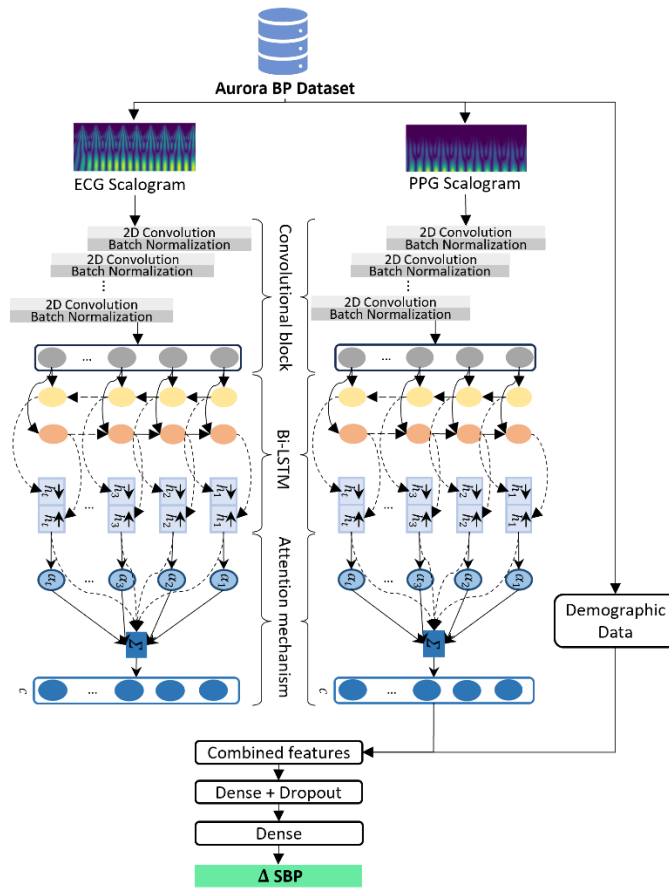# S0. Extended Multimodal Universal Neural Network Architecture

Figure above illustrates the universal model architecture designed for beat-to-beat systolic blood pressure change (ΔSBP) prediction using multimodal physiological inputs. The model accepts CWT-based scalograms derived from ECG and PPG signals as inputs, along with subject-specific demographic features. Each physiological modality is processed independently through a series of three 2D convolutional layers, each followed by batch normalization and ReLU activation. These convolutional blocks extract localized spatial features from the time–frequency representations, allowing the network to capture transient spectral patterns such as heart rate variability and pulse morphology dynamics. The output of each convolutional stream is flattened along the spatial dimensions and passed through a Bidirectional Long Short-Term Memory (BiLSTM) layer, which models temporal dependencies in both forward and backward directions. A temporal attention mechanism is applied on top of the BiLSTM outputs, generating a context vector that emphasizes time steps contributing most significantly to the prediction. Demographic features (e.g., age, sex, injury level) are processed in parallel through a separate dense layer to generate a low-dimensional embedding. This embedding is concatenated with the attention-based context vectors from both ECG and PPG streams in a late-fusion strategy. The fused feature vector is passed through a two-layer fully connected regression head to predict ΔSBP, Dropout and batch normalization are applied to mitigate overfitting. The architecture is trained end-to-end using the mean squared error loss and optimized with the Adam optimizer. This model forms the base architecture for subsequent transfer learning to the SCI cohort, as detailed in the main manuscript.

S0. References

[1] Z.-M. Zhang, S. Chen, and Y.-Z. Liang, "Baseline correction using adaptive iteratively reweighted penalized least squares," Analyst, vol. 135, no. 5, pp. 1138–1146, 2010.

[2] J. Lin and L. Qu, "Feature extraction based on morlet wavelet and its application for mechanical fault diagnosis," Journal of sound and vibration, vol. 234, no. 1, pp. 135–148, 2000.

[3] O. Faust, Y. Hagiwara, T. J. Hong, O. S. Lih, and U. R. Acharya, "Deep learning for healthcare applications based on physiological signals: A review," Computer methods and programs in biomedicine, vol. 161, pp. 1–13, 2018

[4] Whelton, P. K., Carey, R. M., Aronow, W. S., et al. (2018). 2017 ACC/AHA/AAPA/ABC/ACPM/AGS/APhA/ASH/ASPC/NMA/PCNA guideline for the prevention, detection, evaluation, and management of high blood pressure in adults. *Journal of the American College of Cardiology*, 71(19), e127–e248.